Quantum Dots Based Photocatalytic Hydrogen Evolution

Xiang-Bing Fan,[a] Shan Yu,[b] Bo Hou*,[a] and Jong Min Kim[a]

Abstract: Photocatalytic production of hydrogen from water can directly convert solar energy into chemical energy storage, which has significant advantages and great promise. As an emerging photosensitizer, the efficiency of quantum dots (QDs) based artificial photosynthetic system have made breakthroughs. In this review, we will give a summary of the development of QDs based photocatalytic hydrogen evolution in these years. First, we highlight different types of hydrogen evolution catalyst combined with QDs; then we focus on the surface modification and heterostructure formation of QDs to improve the photocatalytic efficiency, respectively. In the end, we will propose some Cd-free QDs and future development of photocatalytic hydrogen evolution.

Keywords: Photocatalysts • Hydrogen evolution • Quantum dots • Solar fuels

1. Introduction

With the increasing energy demands and environmental pollution, the development of new energy is imperative. Conversion of solar energy into chemical fuel as hydrogen from water splitting is one of the best solutions (Figure 1).[1-5] Apart from bulk semiconductors and molecule chromophores, quantum dots (QDs) have emerged as a rising star as photocatalysts.[6-10] QDs are a kind of semiconductor nanocrystals whose radius are less than their exciton Bohr radius.[11, 12] Typically, these QDs has a diameter from 2 nm to 20 nm and the charge carriers in QDs are confined with barriers in three dimensions.[13] The unique structure of QDs makes them useful in many research fields for photonics, electronic and optoelectronic application.[13-19]

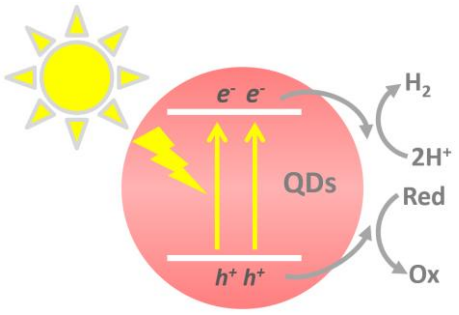

Figure 1. The basic mechanism for QDs based photocatalytic hydrogen evolution. Electrons and holes are generated with light irradiation. Protons are reduced by the photogenerated electrons to generate hydrogen while sacrificial reducing agents (Red) are oxidized by the photogenerated holes to their oxidized forms (Ox).

Especially, QDs have several advantages compared to the traditional materials as photocatalyst.[20, 21] For example, QDs have a variety of parameters that can be used to adjust the bandgap in photocatalysis. Their bandgap increases with the decreasing size of QDs, with the energy level of the conduction band and valence band move up and down, respectively.[12, 21, 22] The enlargement of the bandgap brings more significant driven force for the charge transfer and therefore promote photocatalytic reaction.[23, 24] Besides, the strong quantum-confined effect makes the transport of charge carriers outside the boundary of QDs more easily.[20, 25, 26] Thus, the charge transfer is more efficient in QDs and other quantum-confined structure like nanorods (quantum rod) and nanoplatelets.[20, 27-30] Moreover, multiple photons could be absorbed, and multiple excitons could be generated per QD at the same time.[11, 31] When a hot exciton state is formed when absorbing a photon with $h\nu > 2E_g$, the hot exciton may cool to the band gap, creating one exciton in the lowest energy state, or undergo multiple exciton generation to create two or more excitons.[32] Although the multiple exciton generation is limited in traditional bulk materials, it is greatly enhanced in QDs.[32, 33] Such process could result in quantum efficiency over 100% for energy conversion in photo-related reaction and device.[17] Furthermore, due to the small size of QDs, the ratio of the surface atoms to the total atoms for QDs increase sharply.[22, 34] These surface atoms are incompletely coordinated and usually stabilized by additional surface ligands. Surface atoms, as well as the surface ligands, can influence the whole property of QDs by different surface states. In particular, as electrons and holes need to transfer through the interface of QDs to the outside environment, the surface state of QDs is vital to the performance of photocatalytic reaction.[26, 35]

Because of these unique properties, the reports for QDs based photocatalytic reactions have received increasing interest in recent years. Many types of QDs, such as CdSe, CdTe, CdS, $CuInS_2$ and InP QDs have been successfully applied for efficient hydrogen photogeneration. In this mini-review, we will focus on the progress based on QDs system for photocatalytic hydrogen evolution developed in recent years. From Section 2 to Section 4, we will concentrate on three aspects from the most widely studied II-VI cadmium chalcogenides

[a] X.-B. Fan, B. Hou, J. Kim
Department of Engineering, University of Cambridge
9 JJ Thomson Avenue, Cambridge, CB3 0FA
United Kingdom.
e-mail: bh478@cam.ac.uk
[b] S. Yu
School of Materials Science and Engineering
Southwest Petroleum University
No. 8, Xindu Road, Xindu District, Chengdu, 610500
P. R. China.

QDs systems for photocatalytic hydrogen: the selection of catalyst, the modification of surface and the construction of heterostructure for QDs. In Section 5, we will introduce recent progress involving Cd-free QDs for photocatalytic hydrogen evolution. In addition, some quantum-confined one-dimensional colloidal nanocrystals such as nanorods (quantum rods) for photocatalysis are also included in this review.

2. Selection of hydrogen evolution catalyst with QDs

Like the most traditional semiconductor photocatalysts, the photocatalytic hydrogen evolution efficiency of QDs itself is usually limited even in the presence of sacrificial agents. One possible reason is that the photogenerated electron and hole recombine fast before they transfer to the surface and reaction substrate. Other causes may include the large overpotential for hydrogen evolution and the slow kinetics for hydrogen generation on the surface of QDs.[36, 37] The introduction of hydrogen evolution catalyst to extract electron and reduce the overpotential for hydrogen generation was developed accordingly.

2.1. QDs with inorganic hydrogen evolution catalyst

Platinum is well known as one of the best performing catalysts for the hydrogen evolution reaction, requiring negligible overpotential to achieve high reaction rate.[38] Like many reports in traditional photocatalytic materials, the introduction of Pt inorganic nanoparticles as catalyst is a common strategy in QDs based hydrogen evolution systems. It is found that the size, amount and combination method of Pt particles can affect the photocatalytic efficiency for QDs. For example, Heiz and co-workers synthesized different size of Pt cluster and introduced them on CdS quantum rods. They found that the size of Pt had a crucial relationship with photocatalytic efficiency, and the highest efficiency was reached with Pt cluster containing 46 atoms.[39] Further study showed that the size of cluster affected the LUMO energy level of Pt, which in turn affected the two-step electron transfer process from CdS quantum rods to Pt clusters and from Pt clusters to proton (Figure 2). Later, the relationship between the amount of Pt particles on CdSe/CdS nanorods heterostructure and hydrogen evolution efficiency was investigated by Amirav's group.[40] The system with Pt particles at only one tip of nanorods had the best hydrogen evolution efficiency with 27% apparent quantum yield, while the quantum yield was only 18% for the heterostructure with Pt particles existing at both tips of the nanorods. It demonstrated that hydrogen evolution reaction was based on the multi-step electron transfer process, and the intermediates were more likely to interact with each other in the presence of only one catalytic center. Furthermore, Wu *et al.* reported a self-assembly system consisted of polyacrylic acid ligands capped Pt sol with CdSe/CdS QDs for photocatalytic hydrogen evolution.[41] Control experiments showed that the self-assembly of QDs and Pt sol was formed with the help of polyacrylic acid. Transient absorption and time-resolved X-ray absorption spectra showed that the assembled structure facilitated close contact between QDs and Pt sols, realizing fast electron transfer on a picosecond scale and achieving a remarkable 65% internal quantum yield.

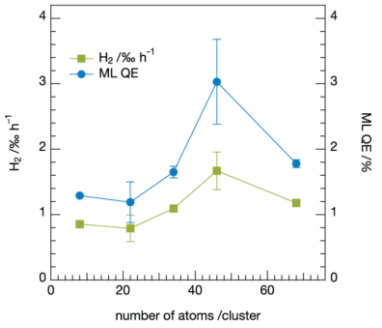

Figure 2. Correlation between the size of the Pt cluster and photocatalytic efficiency. Reprinted with permission from Ref. [39]. Copyright 2013, American Chemical Society.

Due to the scarcity of noble metals, the development of inexpensive hydrogen evolution catalysts is vital for QDs based photocatalysis. It turns out that transition metal ions or their simple inorganic compounds could promote hydrogen evolution as well. In 2013, Wu's group reported photocatalytic hydrogen evolution by direct addition of Co^{2+} ions into CdTe QDs aqueous solution.[42] The (turnover number) TON of 219,100 is obtained related to QDs, with hydrogen evolution rate of 25 μmol h^{-1} mg^{-1}. Under illumination, hollow aggregation nanoparticles were formed by QDs and Co^{2+} ions, which was caused by a hydrogen gas bubble generated in situ as a template (Figure 3).[43] Similar metal ions strategy was also used for photocatalytic hydrogen evolution from water-soluble CdSe and CdS QDs with Ni^{2+}.[44, 45] The catalytic center was formed by the absorption of Ni^{2+} ions on the surface of mercaptopropionic acid capped QDs, and an internal quantum yield of 11.2 % for CdSe QDs (TON 15,340 respect to QDs) and 12.2% for CdS QDs (TON 38,405 respect to QDs) were obtained, respectively.

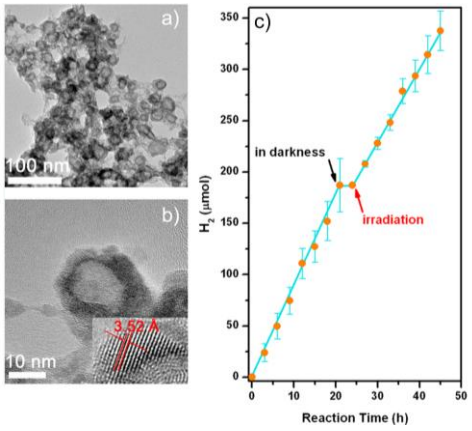

Figure 3. (a-b) HRTEM images of Ni_h-CdTe hollow nanospheres formed by MPA-stabilized CdTe QDs, $NiCl_2 \cdot 6H_2O$, and ascorbic acid under visible light illumination. (c) Photosynthetic H_2 production from Ni_h-CdTe hollow nanospheres. Reprinted with permission from Ref. [43]. Copyright 2014, American Chemical Society.

Feldmann *et al.* realized efficient photocatalytic hydrogen evolution by mixing Ni^{2+} ions and CdS nanorods in highly alkaline aqueous solution.[46] The external quantum yield for

hydrogen evolution exceeds 50% (internal quantum efficiency over 70%) at 447 nm. In particular, the strong alkaline environment shifted the valence band of CdS to a more positive level at which the holes of CdS QDs can produce hydroxyl radicals. These highly active hydroxyl radicals could then react rapidly with sacrificial agents and improve the hydrogen evolution efficiency. Guo's group also brought Ni^{2+} ions into $Cd_{0.5}Zn_{0.5}S$ nanocrystals aqueous solution with Na_2S and Na_2SO_3 as sacrificial agents. Impressively, hydrogen quantum yield of the system at 425 nm is close to 100%.[47] The sub-nanometre NiS_x nanoparticles were formed in situ by Ni^{2+} and S^{2-} ions and freely dispersed in solution without significant interaction with $Cd_{0.5}Zn_{0.5}S$ nanocrystals. Charge transfer from the nanocrystals to NiS_x occurs through the collision between particles, which ensure the efficient electron transfer and meanwhile reduce the back-recombination process. Besides, some new kinds of inorganic transition metal compounds like Co_2C and MoP were also applied in QDs based photocatalysis and obtained satisfactory photocatalytic results.[48, 49]

2.2. QDs with organic hydrogen evolution catalyst

Apart from a lot of work on inorganic catalysts, transition metal-organic complexes (mainly Ni, Co and Fe with organic ligands) are also active hydrogen evolution catalysts in QDs based photocatalytic systems.

In 2012, Eisenberg *et al.* discovered that dihydrolipoic acid ligands on the surface of CdSe QDs could form the catalytic center after complexed with nickel ions (Figure 4).[50] Using ascorbic acid as sacrificial agent, the TON can reach up to 600,000 based on Ni complexes and 1,200,000 based on QDs, respectively. An internal quantum yield of 36% was achieved. Under 520 nm LED illumination, the hydrogen evolution rate had no apparent deactivation with the continuous reaction of 360 h. Later, they found if cobalt ions were introduced instead of nickel ions in the systems, the in-situ formed complex by cobalt ion and dihydrolipoic acid is much less efficient for hydrogen evolution.[51] Subsequently, a series of iron-bis(benzenedithiolate) complexes were used to fulfill photocatalytic hydrogen evolution with CdSe QDs.[52] The hydrogen evolution rate of this system is correlated with the reduction potential of the different iron complexes.

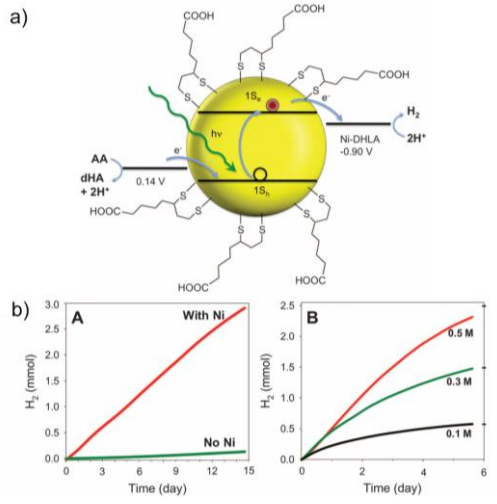

Figure 4. a) Schematic diagram illustrates the relevant energies for H_2 evolution. b) Hydrogen evolution over time from irradiation of dihydrolipoic acid capped CdSe QDs, $Ni(NO_3)_2$, and ascorbic acid. Reprinted with permission from Ref. [50]. Copyright 2012, The American Association for the Advancement of Science.

Chen and co-workers combined cobaloxime complex with CdSe/ZnS QDs to construct photocatalytic hydrogen evolution system.[53] Transient absorption spectra indicated an ultrafast electron transfer from QDs to cobaloxime complex with 105 picosecond, which was much faster than the charge recombination rate. Later, through photoluminescence, transient absorption, and electrochemical spectra analysis, Llobet's group identified the timescale of different processes involved in photocatalytic hydrogen evolution system for CdTe QDs and two kinds of cobalt complexes.[54] The results showed that electron transfer from QDs to cobalt complex was much faster than the back recombination. However, the hydrogen generation rate on cobalt complexes was much slower.

2.3. QDs with Hydrogenase and hydrogenase mimic

Besides the above inorganic and organic materials, the biomimetic study is also applied in QDs photocatalytic system. Natural hydrogenase existed in microorganisms can generate hydrogen from water by irradiation. Hydrogenase has a unique organometallic cluster structure including Fe, Ni, S, C, N and O elements. It can realize hydrogen generation near the H^+/H_2 reduction potential and shows very high hydrogen evolution rate with 6000 - 9000 s^{-1}.[55] As a result, natural hydrogenase or hydrogenase mimetic are promising candidates for QDs based photocatalytic systems.

In 2010, King *et al.* combined the mercaptopropionic acid capped CdTe QDs with the hydrogenases extracted from Clostridium acetobutylicum and realized stable photocatalytic hydrogen evolution.[56] The internal quantum yield reached 9.0% at 532 nm, and the turnover frequency (TOF) of hydrogenase was calculated to be 25 s^{-1}. Subsequently, they introduced the same kind of hydrogenases to CdS colloidal nanorods and realized a higher photocatalytic efficiency with 20% internal quantum yield and TOF of 983 s^{-1} respect to hydrogenases.[57] The improved catalytic efficiency resulted from the good assembly effect between hydrogenases and CdS nanorods. Thus, the electron transfer rate from CdS to hydrogenases was greatly accelerated.[58]

In addition to natural hydrogenases, hydrogenase mimics by artificial synthesis with similar structure are also an interesting field. In 2011, Wu's group reported a photocatalytic system constructed by CdTe QDs and hydrophilic hydrogenase mimics. The TON based on the mimic units reached 505.[59] Later, they introduced chitosan into QDs-hydrogenase mimics system to simulate the restricted environment around the active site of hydrogenase in nature (Figure 5).[60] The hydroxyl and protonated amino group in chitosan had good affinity with both CdTe QDs and hydrogenase mimic for a closer distance, leading hydrogen evolution efficiency 4000-fold higher than that without chitosan. The TON for the hydrogenase mimics in this work had reached 5.28×10^4. Besides CdTe QDs, CdSe QDs can also work with

hydrogenase mimics. By self-assembly at the interface between water and dichloromethane, hydrogenase mimic could be directly loaded on the surface of CdSe QDs.[61] In order to enhance the interaction between CdSe QDs and hydrogenase mimics, polyacrylic acid was introduced further.[62] Polyacrylic acid could not only avoid the aggregation of CdSe QDs but also effectively short the distance between QDs and hydrogenase mimics. Moreover, positive charge polyethyleneimine in the solution could form a second coordination layer in addition to polyacrylic acid, which further promoted the hole transfer process and improved stability of the system during the reaction.[63]

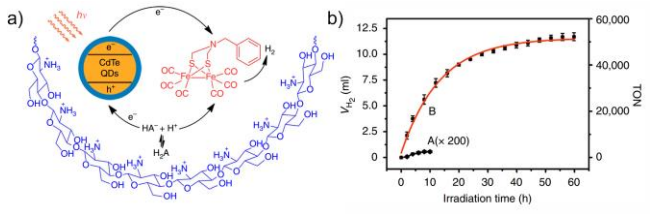

Figure 5. a) Schematic for photocatalytic hydrogen evolution based on CdTe QDs and hydrogenase mimics. b) H_2 evolution under the optimized conditions in the absence (A) and presence (B) of chitosan, containing MPA-CdTe QDs, hydrogenase mimics and H_2A in methanol/water (1:3 v/v) at pH 4.5. Reprinted with permission from a) Ref. [60]. Copyright 2013, Nature Publishing Group.

3. Surface manipulation of QDs for photocatalytic hydrogen evolution

In recent years, the surface state of QDs has been proved to have a direct relationship with photocatalytic performance. With suitable manipulation of the surface state of QDs, photocatalytic hydrogen evolution efficiency can be improved remarkably.

3.1. Manipulation of surface atom ratio on QDs

As a large portion of atoms in QDs exposed on the surface, different surface atom ratio of QDs can modify the photoluminescence property.[64, 65] Recent studies showed that the surface atom ratio could also influence the photocatalytic efficiency. Li and co-works synthesized a series of CdS QDs with different Cd to S ratio.[66] Using steady and time-resolved photoluminescence spectroscopy, they found S/Cd ratio could significantly change the surface state and affect both emissions from the shallow traps and deep traps in CdS. As the charges in the shallow trap were responsible most for photocatalytic hydrogen evolution, the optimized S/Cd ratio with a Cd-rich surface could, therefore, promote the activity for photocatalytic hydrogen evolution. The surface atom ratio was also studied in CdSe QDs.[67, 68] The different surface ratio of Se/Cd also had a significant effect on both the charge transfer and recombination process. With an optimal surface atom ratio, the hole trapping process could be modified for improved photocatalytic hydrogen evolution efficiency.

3.2. Manipulation of surface ligand on QDs

Mostly, the surface atoms on QDs are coordinated with surface ligands, which are indispensable during the QDs synthesis.[69-73] Recent studies showed that these surface ligands could also affect efficiency during photocatalytic hydrogen evolution. In 2013, Eisenberg and co-works found that compared to mono- or bi-coordinate thiol ligands, tri-coordinated thiol ligands on CdSe QDs were more beneficial to maintain the hydrogen evolution stability.[51] Later, Jin's group modified the surface of CdSe/CdS QDs with 2,3-dimercaptosuccinic acid, mercaptopropionic acid, and polyacrylic acid, respectively. These different ligands capped QDs exhibited very different hydrogen evolution rate.[74] Such a variation in the efficiency was mainly caused by the different suppression ability for the surface defects of QDs by these ligands. Apart from thiols, triethanolamine can also work as surface ligands on CdS QDs for photocatalytic hydrogen evolution with the replacement of the original cysteine,[75] though triethanolamine is usually used as an electron sacrificial agent. After the triethanolamine introduction, the photocatalytic hydrogen evolution activity was well maintained within 10 h, much stable than that without triethanolamine. Such an improvement was attributed to the short dendritic chain structure of triethanolamine, which could bind to the surface of CdS QDs and maintain the colloidal dispersion.

On the other hand, by the comparison for a series of mercaptocarboxylate ligands with different length, Dukovic *et al.* found that the rate constant for electron transfer from CdS nanorods to hydrogenases decreased exponentially with the length of surface ligands.[76] Further, Reisner and co-works removed the surface mercaptopropionic acid ligands on CdS QDs. It resulted in a 175 times enhancement for the pristine organic ligands capped ones.[77] The presence of mercaptopropionic acid ligands was not conducive to the bind of catalyst as well as the diffusion of sacrifice agents on the surface of CdS QDs. Besides, the aggregation caused by the removal of mercaptopropionic acid may also promote the charge transfer from one QD to another. Later, they introduced these surface ligands removed CdS QDs into the strongly alkaline solution and got CdS/CdO_x QDs with surface etched by OH^- (Figure 6).[78] Such QDs had been proved to be highly efficient for lignocellulose reforming for hydrogen evolution under irradiation, which demonstrated a new promising photocatalytic application with hydrogen generation of QDs.

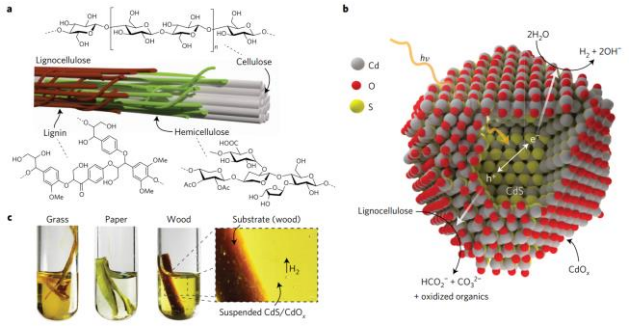

Figure 6. Photoreforming of lignocellulose to H_2 on CdS/CdO_x. a) Lignocellulose existed in plant cell walls and is comprised of cellulose and less crystalline polymers hemicellulose and lignin. b) Photoreforming lignocellulose into H_2 by CdS/CdO_x QDs. c) CdS/CdO_x QDs generate H_2 from crude sources of lignocellulose when suspended in alkaline solution under sunlight irradiation. Reprinted with permission from Ref. [78]. Copyright 2017, Nature Publishing Group.

To keep the colloidal stability of QDs in aqueous solution, inorganic ligands are also used in photocatalysis. In 2014, Jin's group transferred CdS/CdSe QDs into the aqueous solution through inorganic sulfide ions as ligands.[79] Under optimal conditions, the quantum yield for hydrogen evolution could reach 20% at 520 nm. In 2016, Rao *et al.* prepared CdS QDs with S^{2-} by ligand exchange. When using hydrazine hydrate as sacrificial agents, they found that the hydrogen evolution rate of CdS QDs with S^{2-} ligands were 7-8 times higher than that of CdS QDs with mercaptopropionic acid as ligands.[80] Wu's group synthesized CdSe/CdS QDs with S^{2-} ligands by a modified successive ion layer adsorption and reaction method in aqueous solution and achieved a quantum yield of 52% for hydrogen evolution.[81] The inorganic S^{2-} ligands could not only replace native organic ligands and keep colloidal stability in water but also facilitated the direct construction of the CdSe/CdS-$Ni(OH)_2$ photocatalyst in situ. Similarly, S^{2-} capped CdSe/ZnS QDs were also synthesized in aqueous solution and used for photocatalytic hydrogen evolution with MoS_2 as a catalyst.[82]

Obviously, introduce inorganic ions like S^{2-} will create additional surface traps on QDs, which goes against the photoluminescence. However, whether these surface states/traps facilitate or impede on photocatalytic reaction may not be consistent in different systems. Recently, Wu and co-works studied the role of sulfide ions on CdSe QDs in details by gradually increasing the number of sulfide ions in the aqueous solution of QDs. It turned out that the initial sulfide ions mainly grew into the crystal lattices of QDs, and subsequently introduced sulfide ions worked as the ligands.[83] Under optimal condition, the photocatalytic hydrogen evolution activity increased by 4-fold, and TON reached 7,950 for sulfide modified CdSe QDs (Figure 7). In-depth studies showed that lattice sulfide ions were more conducive to electron transfer and ligand sulfide ions primarily promoted holes transfer. Such study reveals the complex role of the surface ions on QDs.

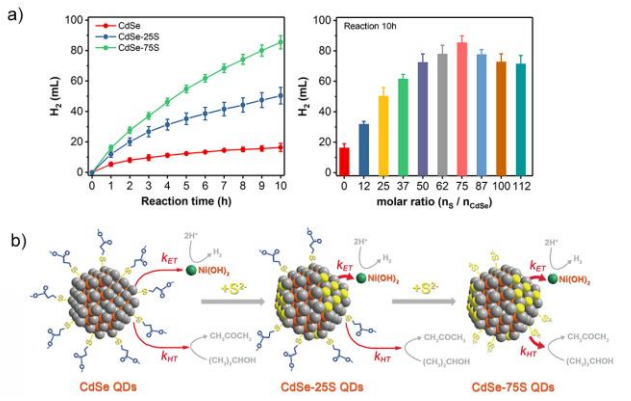

Figure 7. a) Photocatalytic hydrogen evolution for CdSe-*n*S QDs with different ratio of S^{2-} added to CdSe QD solution. b) The propose influence of S^{2-} on mercaptopropionic acid capped CdSe QDs at different stages. Reprinted with permission from Ref. [83]. Copyright 2019, Wiley-VCH.

Considering about the uselessness of organic ligands for the ligand exchange process, Wu's group directly synthesized CdS and CdS/ZnS colloidal nanocrystals with excess sulfide ions in aqueous solution and obtained inspiring photocatalytic hydrogen evolution efficiency with only a small amount of materials used.[84] No organic species were involved during all the synthesis of the colloidal nanocrystal, which avoided unnecessary waste of organic ligands and brought a new way for the design of highly efficient QDs photocatalyst.

4. QDs based heterostructure for photocatalytic hydrogen evolution

Besides the introduction of hydrogen evolution catalyst and surface manipulation, QDs based heterostructure, such as core-shell and dot-in-rod structures, can also help to improve photocatalytic efficiency. Based on the band alignment of the different component in QDs, the QDs based heterostructure can be classified as type-I and type-II. Further, QDs can also form heterostructure with some conventional semiconductors.

4.1. Type-I QDs heterostructure

In type-I QDs heterostructure, the energy level of the conduction band in the shell is more negative than that in the core, while the energy level of the valence band in the shell is more positive than that in the core. Therefore, both the electron and hole are confined to the core.[22, 85] In this case, the shell mainly contributes to reduce the surface defect state of QDs and weaken pathways for the exciton recombination.

Larsen and co-works proposed type-I CdSe/CdS heterostructure QDs by growing a layer of CdS outside the CdSe core. The hydrogen evolution efficiency was then significantly improved (Figure 8).[86] Through transient absorption spectrum, they found many deep trap states existed on the surface of pristine CdSe QDs. These defect states could not produce hydrogen due to their lower energy level. By the growth of CdS, the deep trap states could be effectively passivated. Therefore, more electrons can maintain at the conduction band and participate in the hydrogen evolution reaction. Similarly, type-I CdS/ZnS core-shell QDs were synthesized for efficient and stable photocatalytic hydrogen evolution after loading catalyst.[87] ZnS shell could not only reduce the defect state of CdS QDs by surface passivation but also slow down photocorrosion of CdS. However, the thickness of the shell should not be too thick for photocatalysis. Wu and co-works reported a system by partially covering certain amount of ZnS shell on the surface of CdSe QDs.[88] More than surface passivation, the thin ZnS shell in the system retained the tunneling effect for photoexcited electron and hole to reach the reactive site on the surface of QDs.

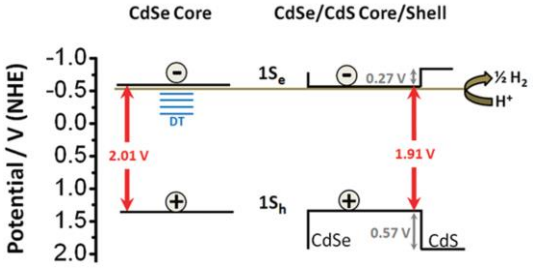

Figure 8. Schematic image shows the removal of CdSe deep trap sites by the CdS shell. Bandgaps were determined via Tauc plots. Reprinted with permission from Ref. [86]. Copyright 2011, American Chemical Society.

Some type-I heterostructure can also realize better charge separation. In these cases, the shell is considered to be the main light absorption material. When the electron is generated at the shell, the hole will transfer to the core for a better charge. For example, Alivisatos *et al.* designed type-I CdSe/CdS heterostructure by growing CdS nanorods on CdSe QDs as seed.[89] With Pt as a catalyst, 20% apparent quantum yield at 450 nm was obtained, which was primarily improved compared with the bare CdSe QDs and the individual CdS nanorods. After exciton formation on CdS rod, the hole would soon transfer to CdSe core, which fulfilled the charge separation spatially. Later, instead of Pt amorphous MoS_3 was loaded on the surface of CdS rods by in situ photoreductions of molybdate.[90] The hydrogen evolution rate of this system could reach 100 mmol h^{-1} g^{-1}, with 10% apparent quantum yield at 450 nm. Apart from traditional type-I heterostructure, Jin and co-works found that reversed type-I CdS/CdSe core-shell QDs could also achieve efficient photocatalytic hydrogen evolution.[91] The reversed type-I heterostructure is formed when the conduction band of the core is more negative than that of the shell, and the valence band of the core is more positive than that of the shell. Such band alignment will promote the electron and hole transfer from the interior core to the outer shell, which is a benefit for the charge extraction for the following photocatalytic reaction.

4.2. Type-II QDs heterostructure

Unlike the type-I QDs heterostructure, the type-II QDs heterostructure establishes through growing shell materials with both the conduction and valence band energy levels more negative or positive than that in the core. Thus, electrons and holes can be confined in the core and shell separately and realized charge separation.

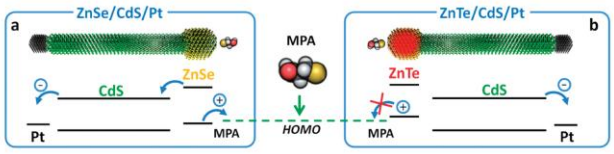

Figure 9. Electronic level diagram showing the different band alignment of excited state energies in ZnSe/CdS/Pt and ZnTe/CdS/Pt heteronanocrystals. Reprinted with permission from Ref. [92]. Copyright 2011, American Chemical Society.

Zamkov's group had designed CdS/ZnSe type-II dot-in-rod heterostructure for photocatalytic hydrogen evolution.[92] As both conduction band and valence band of ZnSe was more negative than that of CdS, electrons accumulated at the conduction band of CdS and holes gathered on the valence band of ZnSe, which realized the effective separation of photogenerated electrons and holes (Figure 9). In contrast, CdS/ZnTe heterostructure could hardly produce hydrogen as holes could not transfer to ZnTe. CdSe/CdS dot-in-rod can also form quasi-type-II heterostructure when the CdSe core has a more negative conduction band than that of CdS (happened when the size of CdSe seed is smaller than 2.7 nm or 3.0 nm), where the electrons are delocalized in the whole structure while the holes are only confined in the CdSe core.[93, 94] Lian *et al.* designed CdSe/CdS dot-in-rod heterostructure as a photosensitizer, methyl viologen as an electron relay, and Pt nanoparticle as a catalyst to achieve efficient electron transfer.[27] For a comprehensive comparison between different structures of CdSe QDs, CdS nanorods, and CdSe/CdS core-shell QDs, they found that the hydrogen evolution rate of all other structures was lower than that of quasi-type-II CdSe/CdS dot-in-rod because of the difference in charge separation efficiency. Later, Zamkov and co-works found that though the holes were confined in the core of quasi-type-II CdSe/CdS nanorod, they were too far away to reach the surface.[93] To overcome this shortcoming, they partly etched CdSe/CdS nanorods to expose more of the inner CdSe core to the surface. For these etched CdSe/CdS, the oxidation reaction rate was much faster and close to the speed of proton reduction, thus increased hydrogen evolution efficiency by 3-4 times. Furthermore, Amirav *et al.* applied CdSe/CdS quasi-type-II dot-in-rod heterostructure into a strongly alkaline solution with Pt as a hydrogen evolution catalyst. Besides the excellent band alignment, they also introduced Pt on one tip of the nanorods and used high concertation of hydroxyl anions for better electrons and holes transfer, respectively. Benefiting for these designs for charge separation, the internal quantum yield for hydrogen evolution was close to 100%.[95]

4.3. QDs heterostructure with traditional semiconductor

In addition to Type-I and Type-II heterostructure, QDs can also be combined with other traditional semiconductors for photocatalysis. For example, CdSe QDs can combine with TiO_2 to improve photocatalytic hydrogen evolution efficiency.[96-98] Using mercaptopropionic acid as a linker, CdSe QDs could attach to commercial TiO_2 effectively. In detail, the thiol group of mercaptopropionic acid was coordinated with Cd atoms on the surface of CdSe QDs, and the carboxyl group was bonded to the Ti atoms on the surface of TiO_2, thereby achieving a close contact between CdSe QDs and TiO_2. Efficient photocatalytic hydrogen evolution could be obtained after further loading $Ni(OH)_2$ on TiO_2 as a catalyst.[98] The study showed that after the QDs excited under visible light irradiation, the photogenerated electrons were firstly transferred to TiO_2 and then further moved to $Ni(OH)_2$ for hydrogen generation. TiO_2 here acted as an electron relay to promote the charge separation.

In addition, polymer graphic carbon nitride (g-C_3N_4) had also been used for photocatalytic hydrogen evolution with QDs. For example, CdS QDs and carbon nitride can directly be combined with physical mixing.[99] Under light illumination, the electrons on g-C_3N_4 transferred to CdS, and the holes on the CdS QDs transferred to g-C_3N_4, which realized charge separation in the space. Similarly, CdSe QDs could form heterostructure with g-C_3N_4.[100] By the proper amount of loading, the photocatalytic efficiency could be improved in contrast to either CdSe QDs or g-C_3N_4 alone.

5. Cd-free QDs for photocatalytic hydrogen evolution

Till now, Cd-based II-VI QDs are the most popular QDs used in photocatalysis. However, the toxicity of Cd may limit their further application. Accordingly, Cd-free QDs are gradually explored for photocatalytic hydrogen evolution, and some of them get impressive results which are comparable to the Cd-based ones.

5.1. ZnSe QDs photocatalyst

Owing to the similar properties between Cd and Zn, the Zn based QDs have also received interest for photocatalyst in these years. Compare to Cd and another metal element in the QDs composition, Zn is rather earth abundant and eco-friendly. Reisner *et al.* demonstrated that ZnSe nanorods were efficient for solar-driven H_2 evolution even without an additional hydrogen evolution catalyst (Figure 10).[101] Besides photocatalytic reaction, they also used ZnSe nanorods to construct photoelectrochemical reaction with $CuCrO_2$. Both photocatalytic and photoelectrochemical hydrogen evolution results showed that the performance of ZnSe approached to that of Cd-based QDs without exhibiting the toxicity, highlighting the potential of Zn based QDs in photocatalysis. Similar, Jia's group showed the photocatalytic ability for nearly monodisperse colloidal ZnS_xSe_{1-x} quantum rods, which were synthesized by alkyl-thiol etching from polydisperse ZnSe nanowires.[102] Compared with sole ZnS and ZnSe, alloyed ZnS_xSe_{1-x} quantum rods showed enhanced photocatalytic activity because of the highly active Zn site on the (100) surface.

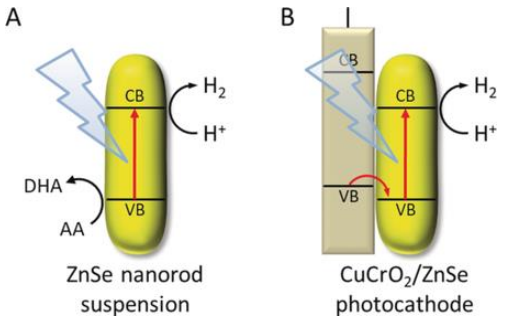

Figure 10. Schematic representation of the ZnSe nanorods photocatalytic and photoelectrochemical system (CB: conduction band, VB: valence band, AA: ascorbic acid, DHA: dehydroascorbic acid). Reprinted with permission from Ref. [101]. Copyright 2019, Wiley-VCH.

5.2. Multinary chalcogenide semiconductors QDs photocatalyst

Multinary chalcogenide QDs belong to ternary I-III-VI semiconductor are also one of the possible less toxic alternatives.[103] These I-III-VI based ternary or quaternary QDs have shown the promising result in photocatalysis in many reports.[104] In 2013, Teng *et al.* tried $CuInS_2$ QDs for photocatalytic hydrogen evolution.[105] The as-prepared $CuInS_2$ QDs had a size about 4.3 nm and a bandgap of 1.97 eV with its conduction band located at -1.2 V (vs. NHE), which made it thermodynamics feasible for hydrogen evolution. After photodeposition of Ru on the surface, 4.7% apparent quantum yield was achieved. Moreover, additional ZnS shell can be applied on the $CuInS_2$ QDs for surface passivation, which is similar to Cd-based type-I heterostructure QDs.[106, 107]

One interesting property of these alloyed chalcogenide QDs is that their bandgap can not only be tuned by the size, but also by the composition of QDs. And it is easy to speculate that the bandgap of QDs has a large influence on photocatalytic efficiency. Generally, the influence of light absorption and driving force for charge transfer are opposed. A wide bandgap promotes electron/hole transfer while leading to less efficient light absorption, and vice versa. A well-adapted bandgap for photocatalyst should balance both trends. In these multinary QDs, the bandgap can be well tuned by the different compositions and affect the photocatalytic efficiency. Wu's group synthesized a series of non-stoichiometric Cu-In-S QDs and found that the In-rich Cu-In-S QDs presented much better photocatalytic result.[108] The optimized ratio of In to Cu in these QDs was 6:1, with an internal quantum yield of 20% for hydrogen evolution under visible-light irradiation. Besides the tune of Cu and In ratio, the introduction of the fourth element into $CuInS_2$ QDs could make the bandgap tunable much easier by different composition and further improve the photocatalytic efficiency.[109] Analogously, Ga could also be incorporated into $CuInS_2$ QDs.[110] Studies show that the fourth incorporated element can also help to reduce the surface state in some cases. Ning *et al.* discovered that in addition to the bandgap adjustment of QDs, the introduction of Zn into $CuInS_2$ QDs could further reduce defect states which are originated from Cu vacancies.[111] Such a decrease in defect states could be well explained by DFT calculation, where they found that formation energy on defect state in $ZnCuInS_2$ QDs was much larger than that of $CuInS_2$.

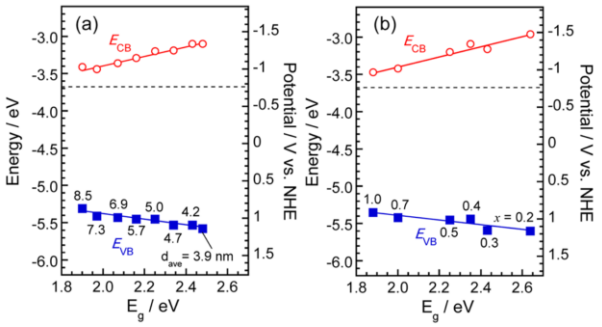

Figure 11. Electronic energy diagrams of the conduction band (open circles) and valence band (solid squares) as a function of the bandgap. Samples were a) Zn-Ag-In-S (Zn_2AgInS_4) QDs with different diameter and (b) $(AgIn)_xZn_{2(1-x)}S_2$ NCs prepared at various x values with d_{ave} of ca. 5 nm. The dotted lines indicate energy level for hydrogen evolution of pH 12.8 in aqueous solution. Reprinted with permission from Ref. [115]. Copyright 2015, American Chemical Society.

Similar to Cu-based one, Ag-In-Zn-S QDs are applied in photocatalytic hydrogen evolution as well.[112-116] Zou *et al.* found that $(AgIn)_xZn_{(1-x)}S_2$ QDs with a x value of 0.5 had the highest efficiency, and the apparent quantum efficiency was 8.2% at 450 nm.[114] Torimoto and co-works noted that the bandgap of the Ag-In-Zn-S QDs could not only be adjusted by the different ratio of $AgInS_2$ and ZnS, but also by the size control of QDs with different amount of 1-dodecanethiol introduced during synthesis (Figure 11).[115] Ning's group further put Zn-Ag-In-S QDs on the MoS_2 2D nanosheet for photocatalytic hydrogen evolution and achieved an excellent external quantum efficiency of 40.8% at 400 nm.[116] Such a high efficiency came from two aspects. First was the heterostructure formation between QDs and MoS_2 2D nanosheets combined the strong light harvesting capability of QDs with the excellent catalytic performance of MoS_2. The second was the dramatical decrease of the deep energy level defects in QDs, which

was fulfilled by compositional engineering through the different amount of Zn incorporation.

5.3. III-VI QDs photocatalyst

InP QDs are new attractive material for solar energy conversion. In comparison to the widely investigated CdSe QDs, InP has smaller bulk band gap (1.35 eV vs. 1.76 eV) and larger Bohr exciton radius (9.6 nm vs. 4.6 nm), which widens its absorption range.[117] Furthermore, InP is more suited for the environmental application than Cd based QDs.[117] After a breakthrough in photoelectrode and solar cell,[118, 119] InP QDs have been successfully employed for photocatalytic reaction very recently. Greta and Wu *et al.* utilized sulfide capped InP and InP/ZnS QDs for photocatalytic hydrogen evolution (Figure 12).[120] The hydrogen evolution rate of InP QDs could be comparable to that of CdSe QDs. When ZnS was covered on the surface of InP QDs, the efficiency was higher. Under optimal condition, the internal quantum yield of 31% at 525 nm was obtained. Furthermore, control experiments showed that sulfide ions on the surface outperformed a series of other organic and inorganic ligands for hydrogen evolution. In-depth mechanism study showed that these sulfide ions ligands could act as a hole transfer relay between QDs and the reaction medium, thus promote the charge separation efficiency.

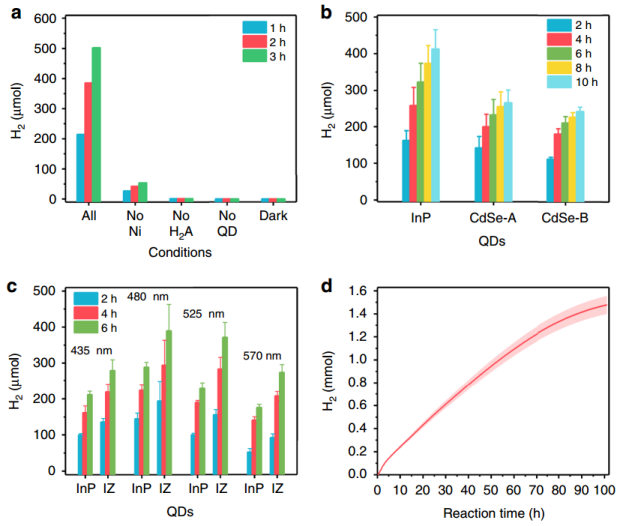

Figure 12. Photocatalytic hydrogen evolution experiments for InP based QDs. a) Photocatalytic control experiment without Ni^{2+}, H_2A, QDs or light illumination, respectively. b) Comparison of hydrogen evolution results with InP QDs and two kinds of CdSe QDs. c) Hydrogen evolution with InP QDs and InP/ZnS QDs (abbreviated as IZ) with different sizes. d) Long time hydrogen evolution of InP/ZnS QDs (shadowed area: error range). Reprinted with permission from Ref. [120]. Copyright 2018, Nature Publishing Group.

Later, Pillai's group also showed the efficient photocatalytic ability of InP/ZnS QDs through two different classes of redox reactions as metal-centered and C-C bond formation.[121] By tuning the surface ligands, InP/ZnS QD could enable different photocatalytic reaction in aqueous solution as well as in organic media. The excellent overlap of the efficiency in different wavelength and the absorption spectra confirmed the active participation of QDs in photocatalysis, further demonstrated the potential of InP QDs for photocatalytic application.

6. Outlook

In this mini-review, the progress of QDs based photocatalytic hydrogen evolution system is briefly discussed. Various research groups established a series of high-efficiency photocatalytic hydrogen evolution system based on QDs.

However, the QDs based photocatalytic hydrogen evolution is still under challenge in many aspects. For example, how to further improve efficiency and keep stability at the same time. Future study may be focused on the exploitation of new kind of stable QDs as well as some cheap but efficient hydrogen evolution catalysts. The dynamic process in excited QDs should also be revealed more clearly, and more efforts should be made for the promotion of charge transfer and suppression of charge recombination.

Besides, it is worth mentioning that the QDs based photocatalysis are mainly focused on the hydrogen evolution half-reaction with the existence of sacrificial agents, which is still far away from practical application. More biomass reforming works may be a direction for QDs based photocatalytic hydrogen evolution study, and overall water splitting on QDs is also urgent for the future development.

Acknowledgments

This work was supported by the European Research Council (ERC Advance No. 340538, Horizon 2020 No. 685758) and EPSRC (EP/P027628/1). B. H. would like to acknowledge EPSRC (EP/K040375/1) for funding the 'South of England Analytical Electron Microscope' used in his research.

References

[1] S. Chu, Y. Cui, N. Liu, *Nat Mater* **2017**, *16*, 16-22.
[2] T. Hisatomi, J. Kubota, K. Domen, *Chem. Soc. Rev.* **2014**, *43*, 7520-7535.
[3] S. Berardi, S. Drouet, L. Francas, C. Gimbert-Surinach, M. Guttentag, C. Richmond, T. Stoll, A. Llobet, *Chem. Soc. Rev.* **2014**, *43*, 7501-7519.
[4] A. Kudo, Y. Miseki, *Chem. Soc. Rev.* **2009**, *38*, 253-278.
[5] X. Chen, S. Shen, L. Guo, S. S. Mao, *Chem. Rev.* **2010**, *110*, 6503-6570.
[6] Z. Han, R. Eisenberg, *Acc. Chem. Res.* **2014**, *47*, 2537-2544.
[7] L.-Z. Wu, B. Chen, Z.-J. Li, C.-H. Tung, *Acc. Chem. Res.* **2014**, *47*, 2177-2185.
[8] G. Chethana, L. Anna, B. Raffaella, *J. Phys. D: Appl. Phys.* **2017**, *50*, 074006.
[9] X.-B. Li, C.-H. Tung, L.-Z. Wu, *Nat. Rev. Chem.* **2018**, *2*, 160-173.
[10] M. S. Kodaimati, K. P. McClelland, C. He, S. Lian, Y. Jiang, Z. Zhang, E. A. Weiss, *Inorg. Chem.* **2018**, *57*, 3659-3670.

[11] A. J. Nozik, M. C. Beard, J. M. Luther, M. Law, R. J. Ellingson, J. C. Johnson, *Chem. Rev.* **2010**, *110*, 6873-6890.

[12] X. Peng, *Acc. Chem. Res.* **2010**, *43*, 1387-1395.

[13] D. V. Talapin, J.-S. Lee, M. V. Kovalenko, E. V. Shevchenko, *Chem. Rev.* **2010**, *110*, 389-458.

[14] K. V. Vokhmintcev, P. S. Samokhvalov, I. Nabiev, *Nano Today* **2016**, *11*, 189-211.

[15] B. Hou, Y. Cho, B.-S. Kim, D. Ahn, S. Lee, J. B. Park, Y.-W. Lee, J. Hong, H. Im, S. M. Morris, J. I. Sohn, S. Cha, J. M. Kim, *J. Mater, Chem. C* **2017**, *5*, 3692-3698.

[16] B. Hou, Y. Cho, B. S. Kim, J. Hong, J. B. Park, S. J. Ahn, J. I. Sohn, S. Cha, J. M. Kim, *ACS Energy Lett.* **2016**, *1*, 834-839.

[17] Y. Yan, R. W. Crisp, J. Gu, B. D. Chernomordik, G. F. Pach, Ashley R. Marshall, J. A. Turner, M. C. Beard, *Nat. Energy* **2017**, *2*, 17052.

[18] A. Nag, M. V. Kovalenko, J.-S. Lee, W. Liu, B. Spokoyny, D. V. Talapin, *J. Am. Chem. Soc.* **2011**, *133*, 10612-10620.

[19] M. Yuan, M. Liu, E. H. Sargent, *Nat. Energy* **2016**, *1*, 16016.

[20] K. Wu, T. Lian, *Chem. Soc. Rev.* **2016**, *45*, 3781-3810.

[21] P. Zrazhevskiy, M. Sena, X. Gao, *Chem. Soc. Rev.* **2010**, *39*, 4326-4354.

[22] A. M. Smith, S. Nie, *Acc. Chem. Res.* **2009**, *43*, 190-200.

[23] M. A. Holmes, T. K. Townsend, F. E. Osterloh, *Chem. Commun.* **2012**, *48*, 371-373.

[24] J. Zhao, M. A. Holmes, F. E. Osterloh, *ACS Nano* **2013**, *7*, 4316-4325.

[25] H. Zhu, Y. Yang, K. Wu, T. Lian, *Annu. Rev. Phys. Chem.* **2016**, *67*, 259-281.

[26] R. D. Harris, S. Bettis Homan, M. Kodaimati, C. He, A. B. Nepomnyashchii, N. K. Swenson, S. Lian, R. Calzada, E. A. Weiss, *Chem. Rev.* **2016**, *116*, 12865-12919.

[27] H. Zhu, N. Song, H. Lv, C. L. Hill, T. Lian, *J. Am. Chem. Soc.* **2012**, *134*, 11701-11708.

[28] C. Liu, F. Qiu, J. J. Peterson, T. D. Krauss, *J Phys. Chem. B* **2014**, *119*, 7349-7357.

[29] S. Lian, D. J. Weinberg, R. D. Harris, M. S. Kodaimati, E. A. Weiss, *ACS Nano* **2016**, *10*, 6372-6382.

[30] Q. Li, F. Zhao, C. Qu, Q. Shang, Z. Xu, L. Yu, J. R. McBride, T. Lian, *J. Am. Chem. Soc.* **2018**, *140*, 11726-11734.

[31] A. J. Nozik, *Chem. Phys. Lett.* **2008**, *457*, 3-11.

[32] M. C. Beard, *J. Phys. Chem. Lett.* **2011**, *2*, 1282-1288.

[33] H. Zhu, Y. Yang, T. Lian, *Acc. Chem. Res.* **2013**, *46*, 1270-1279.

[34] M. A. Boles, D. Ling, T. Hyeon, D. V. Talapin, *Nat. Mater.* **2016**, *15*, 141-153.

[35] E. A. Weiss, *ACS Energy Lett.* **2017**, *2*, 1005-1013.

[36] J. Yang, D. Wang, H. Han, C. Li, *Acc. Chem. Res.* **2013**, *46*, 1900-1909.

[37] J. Ran, J. Zhang, J. Yu, M. Jaroniec, S. Z. Qiao, *Chem. Soc. Rev.* **2014**, *43*, 7787-7812.

[38] Z. W. Seh, J. Kibsgaard, C. F. Dickens, I. Chorkendorff, J. K. Nørskov, T. F. Jaramillo, *Science* **2017**, *355*, 4998.

[39] F. F. Schweinberger, M. J. Berr, M. Döblinger, C. Wolff, K. E. Sanwald, A. S. Crampton, C. J. Ridge, F. Jäckel, J. Feldmann, M. Tschurl, U. Heiz, *J. Am. Chem. Soc.* **2013**, *135*, 13262-13265.

[40] Y. Nakibli, P. Kalisman, L. Amirav, *J. Phys. Chem. Lett.* **2015**, *6*, 2265-2268.

[41] X.-B. Li, Y.-J. Gao, Y. Wang, F. Zhan, X.-Y. Zhang, Q.-Y. Kong, N.-J. Zhao, Q. Guo, H.-L. Wu, Z.-J. Li, Y. Tao, J.-P. Zhang, B. Chen, C.-H. Tung, L.-Z. Wu, *J. Am. Chem. Soc.* **2017**, *139*, 4789-4796.

[42] Z.-J. Li, X.-B. Li, J.-J. Wang, S. Yu, C.-B. Li, C.-H. Tung, L.-Z. Wu, *Energy Environ. Sci.* **2013**, *6*, 465-469.

[43] Z.-J. Li, X.-B. Fan, X.-B. Li, J.-X. Li, C. Ye, J.-J. Wang, S. Yu, C.-B. Li, Y.-J. Gao, Q.-Y. Meng, C.-H. Tung, L.-Z. Wu, *J. Am. Chem. Soc.* **2014**, *136*, 8261-8268.

[44] Z.-J. Li, J.-J. Wang, X.-B. Li, X.-B. Fan, Q.-Y. Meng, K. Feng, B. Chen, C.-H. Tung, L.-Z. Wu, *Adv. Mater.* **2013**, *25*, 6613-6618.

[45] J.-J. Wang, Z.-J. Li, X.-B. Li, X.-B. Fan, Q.-Y. Meng, S. Yu, C.-B. Li, J.-X. Li, C.-H. Tung, L.-Z. Wu, *ChemSusChem* **2014**, *7*, 1468-1475.

[46] T. Simon, N. Bouchonville, M. J. Berr, A. Vaneski, A. Adrović, D. Volbers, R. Wyrwich, M. Döblinger, A. S. Susha, A. L. Rogach, F. Jäckel, J. K. Stolarczyk, J. Feldmann, *Nat Mater* **2014**, *13*, 1013-1018.

[47] M. Liu, Y. Chen, J. Su, J. Shi, X. Wang, L. Guo, *Nat. Energy* **2016**, *1*, 16151.

[48] S. Yin, J. Han, Y. Zou, T. Zhou, R. Xu, *Nanoscale* **2016**.

[49] Q. Guo, F. Liang, X.-Y. Gao, Q.-C. Gan, X.-B. Li, J. Li, Z.-S. Lin, C.-H. Tung, L.-Z. Wu, *ACS Catal.* **2018**, 5890-5895.

[50] Z. Han, F. Qiu, R. Eisenberg, P. L. Holland, T. D. Krauss, *Science* **2012**, *338*, 1321-1324.

[51] A. Das, Z. Han, M. G. Haghighi, R. Eisenberg, *P. Natl. Acad, Sci. USA* **2013**, *110*, 16716-16723.

[52] H. Lv, T. P. A. Ruberu, V. E. Fleischauer, W. W. Brennessel, M. L. Neidig, R. Eisenberg, *J. Am. Chem. Soc.* **2016**, *138*, 11654-11663.

[53] J. Huang, K. L. Mulfort, P. Du, L. X. Chen, *J. Am. Chem. Soc.* **2012**, *134*, 16472-16475.

[54] C. Gimbert-Surinach, J. Albero, T. Stoll, J. Fortage, M. N. Collomb, A. Deronzier, E. Palomares, A. Llobet, *J. Am. Chem. Soc.* **2014**, *136*, 7655-7661.

[55] M. Frey, *ChemBioChem* **2002**, *3*, 153-160.

[56] K. A. Brown, S. Dayal, X. Ai, G. Rumbles, P. W. King, *J. Am. Chem. Soc.* **2010**, *132*, 9672-9680.

[57] K. A. Brown, M. B. Wilker, M. Boehm, G. Dukovic, P. W. King, *J. Am. Chem. Soc.* **2012**, *134*, 5627-5636.

[58] M. B. Wilker, K. E. Shinopoulos, K. A. Brown, D. W. Mulder, P. W. King, G. Dukovic, *J. Am. Chem. Soc.* **2014**, *136*, 4316-4324.

[59] F. Wang, W.-G. Wang, X.-J. Wang, H.-Y. Wang, C.-H. Tung, L.-Z. Wu, *Angew. Chem. Int. Ed.* **2011**, *50*, 3193-3197.

[60] J.-X. Jian, Q. Liu, Z.-J. Li, F. Wang, X.-B. Li, C.-B. Li, B. Liu, Q.-Y. Meng, B. Chen, K. Feng, C.-H. Tung, L.-Z. Wu, *Nat. Commun.* **2013**, *4*, 2695.

[61] C.-B. Li, Z.-J. Li, S. Yu, G.-X. Wang, F. Wang, Q.-Y. Meng, B. Chen, K. Feng, C.-H. Tung, L.-Z. Wu, *Energy Environ. Sci.* **2013**, *6*, 2597-2602.

[62] F. Wang, W.-J. Liang, J.-X. Jian, C.-B. Li, B. Chen, C.-H. Tung, L.-Z. Wu, *Angew. Chem. Int. Ed.* **2013**, *52*, 8134-8138

[63] M. Wen, X.-B. Li, J.-X. Jian, X.-Z. Wang, H.-L. Wu, B. Chen, C.-H. Tung, L.-Z. Wu, *Sci. Rep.* **2016**, *6*, 29851.

[64] H. H.-Y. Wei, C. M. Evans, B. D. Swartz, A. J. Neukirch, J. Young, O. V. Prezhdo, T. D. Krauss, *Nano Lett.* **2012**, *12*, 4465-4471.

[65] J. Jasieniak, P. Mulvaney, *J. Am. Chem. Soc.* **2007**, *129*, 2841-2848.

[66] L. Huang, J. Yang, X. Wang, J. Han, H. Han, C. Li, *Phys. Chem. Chem. Phys.* **2013**, *15*, 553-560.

[67] Y. Ye, X. Wang, S. Ye, Y. Xu, Z. Feng, C. Li, *J. Phys. Chem. C* **2017**, *121*, 17112-17120.

[68] M.-Y. Huang, X.-B. Li, Y.-J. Gao, J. Li, H.-L. Wu, L.-P. Zhang, C.-H. Tung, L.-Z. Wu, *J. Mater. Chem. A* **2018**, *6*, 6015-6021.

[69] L. Li, P. Reiss, *J. Am. Chem. Soc.* **2008**, *130*, 11588-11589.

[70] W. W. Yu, X. Peng, *Angew. Chem. Int. Ed.* **2002**, *41*, 2368-2371.

[71] J. J. Li, Y. A. Wang, W. Guo, J. C. Keay, T. D. Mishima, M. B. Johnson, X. Peng, *J. Am. Chem. Soc.* **2003**, *125*, 12567-12575.

[72] N. C. Anderson, M. P. Hendricks, J. J. Choi, J. S. Owen, *J. Am. Chem. Soc.* **2013**, *135*, 18536-18548.

[73] B. Hou, D. Benito-Alifonso, N. Kattan, D. Cherns, M. C. Galan, D. J. Fermín, *Chem. Eur. J.* **2013**, *19*, 15847-15851.

[74] P. Wang, J. Zhang, H. He, X. Xu, Y. Jin, *Nanoscale* **2015**, *7*, 5767-5775.

[75] W. Li, J. R. Lee, F. Jäckel, *ACS Appl. Mater. Interfaces* **2016**, *8*, 29434-29441.

[76] M. B. Wilker, J. K. Utterback, S. Greene, K. A. Brown, D. W. Mulder, P. W. King, G. Dukovic, *J. Phys. Chem. C* **2017**, *122*, 741-750.

[77] C. M. Chang, K. L. Orchard, B. C. M. Martindale, E. Reisner, *J. Mater. Chem. A* **2016**, *4*, 2856-2862.

[78] D. W. Wakerley, M. F. Kuehnel, K. L. Orchard, K. H. Ly, T. E. Rosser, E. Reisner, *Nat. Energy* **2017**, *2*, 17021.

[79] P. Wang, J. Zhang, H. He, X. Xu, Y. Jin, *Nanoscale* **2014**, *6*, 13470-13475.

[80] M. K. Jana, U. Gupta, C. N. R. Rao, *Dalton Trans.* **2016**, *45*, 15137-15141.

[81] Z.-J. Li, X.-B. Fan, X.-B. Li, J.-X. Li, F. Zhan, Y. Tao, X. Zhang, Q.-Y. Kong, N.-J. Zhao, J.-P. Zhang, C. Ye, Y.-J. Gao, X.-Z. Wang, Q.-Y. Meng, K. Feng, B. Chen, C.-H. Tung, L.-Z. Wu, *J. Mater. Chem. A* **2017**, *5*, 10365-10373.

[82] X.-B. Li, Y.-J. Gao, H.-L. Wu, Y. Wang, Q. Guo, M.-Y. Huang, B. Chen, C.-H. Tung, L.-Z. Wu, *Chem. Commun.* **2017**, *53*, 5606-5609.

[83] X.-B. Fan, S. Yu, X. Wang, Z.-J. Li, F. Zhan, J.-X. Li, Y.-j. Gao, A.-D. Xia, Y. Tao, X.-B. Li, L.-P. Zhang, C.-H. Tung, L.-Z. Wu, *Adv. Mater.* **2019**, *31*, 1804872.

[84] X.-B. Fan, S. Yu, H.-L. Wu, Z.-J. Li, Y.-J. Gao, X.-B. Li, L.-P. Zhang, C.-H. Tung, L.-Z. Wu, *J. Mater. Chem. A* **2018**, *6*, 16328-16332.

[85] H. Zhu, N. Song, T. Lian, *J. Am. Chem. Soc.* **2010**, *132*, 15038-15045.

[86] A. Thibert, F. A. Frame, E. Busby, M. A. Holmes, F. E. Osterloh, D. S. Larsen, *J. Phys. Chem. Lett.* **2011**, *2*, 2688-2694.

[87] L. Huang, X. Wang, J. Yang, G. Liu, J. Han, C. Li, *J. Phys. Chem. C* **2013**, *117*, 11584-11591.

[88] Y.-J. Gao, X.-B. Li, H.-L. Wu, S.-L. Meng, X.-B. Fan, M.-Y. Huang, Q. Guo, C.-H. Tung, L.-Z. Wu, *Adv. Funct. Mater.* **2018**, *28*, 1801769.

[89] L. Amirav, A. P. Alivisatos, *J. Phys. Chem. Lett.* **2010**, *1*, 1051-1054.

[90] M. L. Tang, D. C. Grauer, B. Lassalle-Kaiser, V. K. Yachandra, L. Amirav, J. R. Long, J. Yano, A. P. Alivisatos, *Angew. Chem. Int. Ed.* **2011**, *50*, 10203-10207.

[91] P. Wang, M. Wang, J. Zhang, C. Li, X. Xu, Y. Jin, *ACS Appl. Mater. Interfaces* **2017**, *9*, 35712-35720.

[92] K. P. Acharya, R. S. Khnayzer, T. O'Connor, G. Diederich, M. Kirsanova, A. Klinkova, D. Roth, E. Kinder, M. Imboden, M. Zamkov, *Nano Lett.* **2011**, *11*, 2919-2926.

[93] E. Khon, K. Lambright, R. S. Khnayzer, P. Moroz, D. Perera, E. Butaeva, S. Lambright, F. N. Castellano, M. Zamkov, *Nano Lett.* **2013**, *13*, 2016-2023.

[94] K. Wu, L. J. Hill, J. Chen, J. R. McBride, N. G. Pavlopolous, N. E. Richey, J. Pyun, T. Lian, *ACS Nano* **2015**, *9*, 4591-4599.

[95] P. Kalisman, Y. Nakibli, L. Amirav, *Nano Lett.* **2016**, *16*, 1776-1781.

[96] S. Lee, K. Lee, W. D. Kim, S. Lee, D. J. Shin, D. C. Lee, *J. Phys. Chem. C* **2014**, *118*, 23627-23634.

[97] W. Chen, S. Yu, Y. Zhong, X.-B. Fan, L.-Z. Wu, Y. Zhou, *New J. Chem.* **2018**, *42*, 4811-4817.

[98] S. Yu, Z.-J. Li, X.-B. Fan, J.-X. Li, F. Zhan, X.-B. Li, Y. Tao, C.-H. Tung, L.-Z. Wu, *ChemSusChem* **2015**, *8*, 642-649.

[99] L. Ge, F. Zuo, J. Liu, Q. Ma, C. Wang, D. Sun, L. Bartels, P. Feng, *J. Phys. Chem. C* **2012**, *116*, 13708-13714.

[100] Y. Zhong, W. Chen, S. Yu, Z. Xie, S. Wei, Y. Zhou, *ACS Omega* **2018**, *3*, 17762-17769.

[101] M. F. Kuehnel, C. E. Creissen, C. D. Sahm, D. Wielend, A. Schlosser, K. L. Orchard, E. Reisner, *Angew. Chem. Int. Ed.* **2019**, *58*, 5059-5063.

[102] D. Chen, H. Zhang, Y. Li, Y. Pang, Z. Yin, H. Sun, L.-C. Zhang, S. Wang, M. Saunders, E. Barker, G. Jia, *Adv. Mater.* **2018**, *30*, 1803351.

[103] J. Kolny-Olesiak, H. Weller, *ACS Appl. Mater. Interfaces* **2013**, *5*, 12221-12237.

[104] M. D. Regulacio, M.-Y. Han, *Acc. Chem. Res.* **2016**, *49*, 511-519.

[105] T.-L. Li, C.-D. Cai, T.-F. Yeh, H. Teng, *J. Alloys Compd.* **2013**, *550*, 326-330.

[106] Y. Zhou, W. Hu, J. Ludwig, J. Huang, *J. Phys. Chem. C* **2017**, *121*, 19031-19035.

[107] M. Sandroni, R. Gueret, K. D. Wegner, P. Reiss, J. Fortage, D. Aldakov, M. N. Collomb, *Energy Environ. Sci.* **2018**, *11*, 1752-1761.
[108] X.-B. Fan, S. Yu, F. Zhan, Z.-J. Li, Y.-J. Gao, X.-B. Li, L.-P. Zhang, Y. Tao, C.-H. Tung, L.-Z. Wu, *ChemSusChem* **2017**, *10*, 4833-4838.
[109] B. Zhang, Y. Wang, C. Yang, S. Hu, Y. Gao, Y. Zhang, Y. Wang, H. V. Demir, L. Liub, K.-T. Yong, *Phys. Chem. Chem. Phys.* **2015**, *17*, 25133-25141.
[110] T. A. Kandiel, G. A. M. Hutton, E. Reisner, *Catal. Sci. Technol.* **2016**, *6*, 6536-6541.
[111] X.-Y. Liu, G. Zhang, H. Chen, H. Li, J. Jiang, Y.-T. Long, Z. Ning, *Nano Res.* **2017**, *11*, 1379-1388.
[112] M. Jagadeeswararao, S. Dey, A. Nag, C. N. R. Rao, *J. Mater. Chem. A* **2015**, *3*, 8276-8279.
[113] G. Gong, Y. Liu, B. Mao, L. Tan, Y. Yang, W. Shi, *Appl. Catal., B* **2017**, *216*, 11-19.
[114] Y.-J. Yuan, D.-Q. Chen, M. Xiong, J.-S. Zhong, Z.-Y. Wan, Y. Zhou, S. Liu, Z.-T. Yu, L.-X. Yang, Z.-G. Zou, *Appl. Catal., B* **2017**, *204*, 58-66.
[115] T. Kameyama, T. Takahashi, T. Machida, Y. Kamiya, T. Yamamoto, S. Kuwabata, T. Torimoto, *J. Phys. Chem. C* **2015**, *119*, 24740-24749.
[116] X.-Y. Liu, H. Chen, R. Wang, Y. Shang, Q. Zhang, W. Li, G. Zhang, J. Su, C. T. Dinh, F. P. G. de Arquer, J. Li, J. Jiang, Q. Mi, R. Si, X. Li, Y. Sun, Y.-T. Long, H. Tian, E. H. Sargent, Z. Ning, *Adv. Mater.* **2017**, *29*, 1605646.
[117] G. Fan, C. Wang, J. Fang, *Nano Today* **2014**, *9*, 69-84.
[118] T. Nann, S. K. Ibrahim, P.-M. Woi, S. Xu, J. Ziegler, C. J. Pickett, *Angew. Chem. Int. Ed.* **2010**, *49*, 1574-1577.
[119] J. Wallentin, N. Anttu, D. Asoli, M. Huffman, I. Åberg, M. H. Magnusson, G. Siefer, P. Fuss-Kailuweit, F. Dimroth, B. Witzigmann, H. Q. Xu, L. Samuelson, K. Deppert, M. T. Borgström, *Science* **2013**, *339*, 1057-1060.
[120] S. Yu, X.-B. Fan, X. Wang, J. Li, Q. Zhang, A. Xia, S. Wei, L.-Z. Wu, Y. Zhou, G. R. Patzke, *Nat. Commun.* **2018**, *9*, 4009.
[121] I. N. Chakraborty, S. Roy, G. Devatha, A. Rao, P. P. Pillai, *Chem. Mater.* **2019**, *31*, 2258-2262.

Received: ((will be filled in by the editorial staff))
Accepted: ((will be filled in by the editorial staff))
Published online: ((will be filled in by the editorial staf

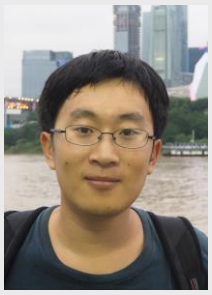

Xiangbing Fan received his B.S. degree in chemistry from Wuhan University in 2012, and her Ph.D. degree from Technical Institute of Physics and Chemistry, Chinese Academy of Science in 2018. Now he is working as a postdoctoral researcher at the Department of Engineering, University of Cambridge. His research interests focus on QDs synthesis and QDs based photocatalytic application.

Shan Yu received her B.S. degree in chemistry from Lanzhou University in 2009, and her Ph.D. degree in Technical Institute of Physics and Chemistry, Chinese Academy of Sciences in 2014. She worked as a guest postdoc at the University of Zurich from 2016 to 2017. She is currently a lecturer at Southwest Petroleum University. Her research interests focus on QDs based photocatalytic application.

Bo Hou is a Senior Research Associate in the Department of Engineering at the University of Cambridge. He received his Ph.D. degree in the School of Chemistry at the University of Bristol (2010–2014) and worked as a postdoctoral researcher at the University of Oxford (2014-2018). His research interests include QD synthesis, QD optoelectronics, electron microscopy (TEM) and dynamic charge transfer analysis.

Jong Min Kim was appointed to the 1944 Chair in Electrical Engineering at the University of Cambridge in 2016. He was the Head of Electrical Engineering at the University of Oxford (2012–2015) and Senior Vice President for Technology at Samsung Electronics (1999–2012). He is responsible for a number of world firsts: colloidal QD based LEDs /displays, LED on glass, CNT field emission high definition displays /lightings, and transparent /flexible graphene electrode. He managed commercialization of LCD, PDP, OLED, and LEDs in Samsung. OLED and LEDs were largely started by his team.